1
Proteins Separation and Purification by Expanded Bed Adsorption and Simulated Moving Bed Technology

Ping Li, Pedro Ferreira Gomes, José M. Loureiro, and Alirio E. Rodrigues

1.1
Introduction

Proteins not only play an important role in biology, but also have large potential applications in pharmaceuticals and therapeutics, food processing, textiles and leather goods, detergents, and paper manufacturing. With the development of molecular biology technologies, various kinds of proteins can be prepared from upstream processes and from biological raw materials. However, there exist various proteins and contaminants in these source feedstocks, and the key issue is that proteins can be separated and purified efficiently from the source materials, in order to reduce the production cost of the high-purity protein. The development of techniques and methods for proteins separation and purification has been an essential prerequisite for many of the advancements made in biotechnology.

Most separation and purification protocols require more than one step to achieve the desired level of protein purity. Usually, a three-step separation and purification strategy is presented, which includes capture, intermediate separation and purification, and final polishing during a downstream protein separation and purification process. In the capture step the objectives are to isolate, concentrate, and stabilize the target proteins. During the intermediate separation and purification step the objectives are to remove most of the bulk impurities, such as other proteins and nucleic acids, endotoxins, and viruses. In the polishing step most impurities have already been removed except for trace amounts or closely related substances. The objective is to achieve final purity of protein.

In the capture step, as the primary recovery of proteins, the expanded bed adsorption (EBA) technology has been widely applied to capture proteins directly from crude unclarified source materials, such as, *Escherichia coli* homogenate, yeast, fermentation, mammalian cell culture, milk, and animal tissue extracts [1,2]. The expanded bed is designed in a way that the suspended adsorbent particles capture target protein molecules, while cells, cell debris,

Continuous Processing in Pharmaceutical Manufacturing, First Edition. Edited by Ganapathy Subramanian.

particulate matter, and contaminants pass through the column unhindered. After loading and washing, the bound proteins can be eluted by elution buffer and be concentrated in a small amount of elution solution, apart from the bulk impurities and contaminants in source materials. With specially designed adsorbents and columns, the adsorption behavior in expanded beds is comparable to that in fixed beds. Various applications of EBA technology have been reported from laboratory-scale to pilot-plant and large-scale production [1–9].

During the intermediate purification and final polishing steps, the techniques of the conventional elution chromatography have been applied successfully. A new challenge should be the application of simulated moving bed (SMB) to the separation and purification of proteins. SMB chromatography is a continuous process, which for preparative purposes can replace the discontinuous regime of elution chromatography. Furthermore, the countercurrent contact between fluid and solid phases used in SMB chromatography maximizes the mass transfer driving force, leading to a significant reduction in mobile and stationary phase consumption when compared with elution chromatography [10–14]. Examples of products that are considered for SMB separation and purification are therapeutic proteins, antibodies, nucleosides, and plasmid DNA [15–23].

When the binding capacities of proteins on adsorbent are close to each other, an isocratic SMB mode may be used to separate and purify the proteins, where the adsorbents have the same affinity capacity to proteins in all sections in SMB chromatography. However, usually the binding capacities of proteins are so different that we cannot separate them by the isocratic mode with a reasonable retention time. In conventional elution chromatography, a gradient mode should be used for the separation of proteins. It is most commonly applied in reversed-phase and ion exchange chromatography (IEC), by changing the concentration of the organic solvent and salt in a stepwise gradient or with a linear gradient, respectively. For SMB chromatography, only a stepwise gradient can be formed by introducing a solvent mixture with a lower strength at the feed inlet port compared with the solvent mixture introduced at the desorbent port; then the adsorbents have a lower binding capacity to proteins in sections I and II to improve the desorption, and have a stronger binding capacity in sections III and IV to increase adsorption in SMB chromatography. Some authors state that the solvent consumption by gradient mode can be decreased significantly when compared with isocratic SMB chromatography [17–19,24–29]. Moreover, when a given feed is applied to gradient SMB chromatography, the protein obtained from the extract stream can be enriched if protein has a medium or high solubility in the solution with the stronger solvent strength, while the raffinate protein is not diluted at all [24].

In this chapter, we shall describe the developments made at the Laboratory of Separation and Reaction Engineering (LSRE) for proteins separation and purification by expanded bed chromatography and salt gradient ion exchange simulated moving bed technology.

1.2
Protein Capture by Expanded Bed Technology

1.2.1
Adsorbent Materials

The design of a special adsorbent is a key factor to enhance the efficiency of expanded bed adsorption. The EBA process will be more effective for those adsorbents that have both high-density base matrix and salt-tolerant ligand. The high-density matrix means minimizing dilution arising from biomass or viscosity in feedstock and reducing dilution buffer consumption; the lack of sensitivity of the ligand to ionic strength and salt concentration means there is no need for dilution of feedstock [30–32].

"Homemade" adsorbents are commonly used for research purposes. Agarose and cellulose are the major components utilized on the tailoring of the adsorbents. Table 1.1 shows a list of such adsorbents.

Table 1.1 "Homemade" adsorbents.

Year	Core	Adsorbent	Reference
1994	Crystalline quartz	6% Agarose	[33]
1994	Perfluorocarbon	Polyvinyl alcohol – perfluorodecalin	[34]
1995	Crystalline quartz - Red H-E7B	6% Agarose	[35]
1995	Perfluorocarbon	Polyvinyl alcohol – perfluoropolymer	[36]
1996	Crystalline quartz - Cibacron blue (3GA)	6% Agarose	[37]
1997	Fluoride-modified porous zirconium oxide		[38]
1999	Polyacrylamide gel	Silica	[39]
1999	Glass	Agarose	[40]
2000	Celbeads[a)]	Cellulose	[41]
2000	Stainless steel	Agarose	[30]
2001	Celbeads[a)]	Cellulose	[42]
2001	Nd–Fe–B alloy powder	Agarose	[43]
2002	Stainless steel	6% Agarose	[44]
2002	Stainless steel	6% Agarose	[45]
2002	Crystalline quartz	6% Agarose (Streamline DEAE) modified with a layer of polyacrylic acid (PAA)	[46]
2002	Nd–Fe–B with Cibacron Blue 3GA (CB)	4% Agarose	[47]
2002	Zirconia-silica (ZSA) ZSA - Cibracron Blue (CB)	4% Agarose 4% Agarose	[9]
2003	Zirconia-silica (ZSA)	Agarose	[48]
2003	CB-6AS	Cellulose	[49]
2003	Titanium oxide	Cellulose	[50]

(*continued*)

Table 1.1 (*Continued*)

Year	Core	Adsorbent	Reference
2004	Glass	4% Agarose	[51]
2005	Titanium oxide	Cellulose	[52]
2005	Stainless steel powder	Cellulose	[53]
2006	Stainless steel powder	Cellulose	[54]
2007	Nickel powder	Cellulose	[55]
2007	Tungsten carbide	Cellulose	[56]
2008	Tungsten carbide	Cellulose	[57]
2008	Stainless steel powder with benzylamine (mixed mode)	Cellulose	[58]
2008	Zirconia-silica	Agarose	[59]
2009	Zirconium dioxide	Polyglycidyl methacrylate β-cyclodextrin	[60]
2009	Tungsten carbide	β-Cyclodextrin polymer	[61]
2010	Tungsten carbide	β-Cyclodextrin polymer	[62]
2010	Tungsten carbide	Agarose	[63]
2011	Tungsten carbide	Cellulose	[64]
2012	Nickel (nanoporous)	Agarose	[31]
2012	Zinc (nanoporous)	Agarose	[32]
2013	Tungsten carbide	3% Agarose	[65]
2013	Titanium dioxide	Polyacrylamide-based Cryogel	[66]

a) Celbeads: Rigid spherical macroporous adsorbent beads with surface hydroxyl groups.

The drawback of agarose/cellulose-based adsorbents is their low density. Therefore, EBA adsorbents were developed by incorporating a dense solid material in the beads. Table 1.2 shows a list of commercial adsorbents.

Adsorbents used in EBA have been developed by some major companies as shown in Table 1.3. The name of the adsorbents are influenced by the ligand used, for example, diethylaminoethyl (DEAE), sulphopropyl (SP), quaternary amine (Q), recombinant protein A (r-Protein A), imino diacetic acid (Chelating), multimodal function (Direct CST I), carboxymethyl (CM), sulfopropyl (S) and polyethyleneimine (PEI) [3,30,71].

The trend is to use a dense solid core material to allow processing of higher flow rates and therefore reach a better productivity [30–32].

Streamline DEAE and Streamline SP (specially designed for an expanded bed), are classical ion exchangers, in which binding proteins are primarily based on interactions between charged amino acids on the protein surface and oppositely charged immobilized ligands. Protein retention on an ionic surface of adsorbent can be simply explained by the pI-value (isoelectric point) of a protein. But in practical applications, it is found that these ion exchangers have a lower binding capacity to proteins in high ionic strength and salt concentration feedstock. Streamline Direct CST I is a cation exchanger with multimodal functional groups, which not only takes advantage of electrostatic interaction, but also takes advantage of hydrogen bond interaction and hydrophobic interaction to tightly bind proteins. In other words, the new type of

Table 1.2 Commercial adsorbents.

Year	Core	Adsorbent	Commercialized series	Reference
1995	Crystalline quartz	6% Cross-linked agarose	Streamline DEAE	[67]
1995	Crystalline quartz	6% Cross-linked agarose	Streamline SP	[68]
1996	Crystalline quartz	6% Cross-linked agarose	Streamline DEAE	[69]
1996	Crystalline quartz	6% Cross-linked agarose	Streamline SP	[70]
1996	Crystalline quartz	4% Cross-linked agarose	Streamline r-Protein A	[3]
1997	Crystalline quartz	6% Cross-linked agarose	Streamline DEAE	[71]
1997	Crystalline quartz	6% Cross-linked agarose	Streamline Phenyl	[72]
1998			DEAE Spherodex LS	[73]
1999	Crystalline quartz	Agarose	Streamline DEAE	[74]
			DEAE Spherodex LS	
1999	Crystalline quartz	Agarose	Streamline DEAE	[75]
1999	Crystalline quartz	6% Cross-linked agarose	Streamline SP	[76]
	Crystalline quartz	6% Cross-linked agarose	Streamline DEAE	
	Crystalline quartz	6% Cross-linked agarose	Streamline Chelating	
1999	Crystalline quartz	6% Cross-linked agarose	Streamline SP	[77]
	Crystalline quartz	6% Cross-linked agarose	Streamline Q XL	
2000	Crystalline quartz	6% Cross-linked agarose	Streamline Phenyl	[78]
2000	Crystalline quartz	6% Cross-linked agarose	Streamline Chelating	[79]
2001	Crystalline quartz	6% Cross-linked agarose	Streamline SP	[80]
	Porous ceramic	Hydrogel	S Ceramic HyperD LS	
2001	Crystalline quartz	6% Cross-linked agarose	Streamline DEAE	[81]
			DEAE Spharose FF	
2001	Crystalline quartz	6% Cross-linked agarose	Streamline DEAE	[42]
	Crystalline quartz	6% Cross-linked agarose	Streamline SP	
2001	Crystalline quartz	6% Cross-linked agarose	Streamline SP	[43]
2001	Crystalline quartz	6% Cross-linked agarose	Streamline Q XL	[82]
2001	Crystalline quartz	6% Cross-linked agarose	Streamline SP	[83]
	Crystalline quartz	6% Cross-linked agarose	Streamline DEAE	
2002	Crystalline quartz	6% Cross-linked agarose	Streamline SP	[84]
	Crystalline quartz	6% Cross-linked agarose	Streamline DEAE	
2002	Crystalline quartz	6% Cross-linked agarose	Streamline Quartz Base Matrix	[45]
2002	Crystalline quartz	6% Cross-linked agarose	Streamline SP	[5]
	Crystalline quartz	6% Cross-linked agarose	Streamline Q XL	
2002	Crystalline quartz	6% Cross-linked agarose	Streamline DEAE	[44]
	Crystalline quartz	6% Cross-linked agarose	Streamline Q XL	
	Glass	6% Cross-linked agarose	UFC DEAE/PEI	
2002	Crystalline quartz	6% Cross-linked agarose	Streamline	[9]
	Kieselguhr particles	4% Cross-linked agarose	Macrosorb K4AX	
2003			DEAE Spherodex M	[85]
2003	Crystalline quartz	6% Cross-linked agarose	Streamline DEAE	[86]
2003			DEAE Spharose FF	[7]
	Crystalline quartz	6% Cross-linked agarose	Streamline DEAE	
2004	Crystalline quartz	6% Cross-linked agarose	Streamline SP	[87]
2004	Crystalline quartz	6% Cross-linked agarose	Streamline SP	[13]

(*continued*)

Table 1.2 (*Continued*)

Year	Core	Adsorbent	Commercialized series	Reference
2004	Tungsten carbide	Agarose	Rhobust Fastline SP	[88]
2004	Tungsten carbide	Agarose	Rhobust Fastline SP	[89]
2005	Stainless steel	4% Cross-linked agarose	Streamline Direct CST I	[90]
	Crystalline quartz	6% Cross-linked agarose	Streamline DEAE	
2005	Crystalline quartz	6% Cross-linked agarose	Streamline DEAE	[91]
	Crystalline quartz	6% Cross-linked agarose	Streamline SP	
2006	Stainless steel	4% Cross-linked agarose	Streamline Direct CST I	[92]
2006	Crystalline quartz	6% Cross-linked agarose	Streamline DEAE	[93]
2007	Zirconium oxide	Hydrogel-filled	Q/CM HyperZ	[94]
2007	Stainless steel	Agarose	Streamline Direct HST	[95]
2008	Crystalline quartz Nickel (primed)	6% Cross-linked agarose	Streamline Chelating	[96]
2008	Crystalline quartz	6% Cross-linked agarose	Streamline DEAE	[59]
	Zirconium oxide	Hydrogel-filled	CM-HyperZ	
2009	Stainless steel	Agarose	Streamline Direct HST	[97]
2009	Macroporous acrylic polymer		Amberlite XAD7 HP	[98]
2010	Crystalline quartz	6% Cross-linked agarose	Streamline Chelating	[99]
2010	Crystalline quartz	6% Cross-linked agarose	Streamline Phenyl	[100]
2011	Crystalline quartz	6% Cross-linked agarose	Streamline DEAE	[101]
2011	Zirconium oxide	Hydrogel-filled	CM HyperZ	[102]
2012	Crystalline quartz	6% Cross-linked agarose	Streamline DEAE	[103]
	Crystalline quartz	6% Cross-linked agarose cover with polyvinyl pyrrolidone	Streamline DEAE modified	
2013	Tungsten carbide	6% Cross-linked agarose	Fastline HSA	[104]
	Tungsten carbide	Agarose	MabDirect MM	
	Zirconium oxide	Hydrogel-filled	CM HyperZ	
2013	Crystalline quartz	6% Cross-linked agarose	Streamline Q XL	[105]
2013	Tungsten carbide	Agarose	Rhobust Fastline SP	[106]
2013	Tungsten carbide	Agarose	MabDirect ProteinA	[107]
2013	Tungsten carbide	Agarose	MabDirect MM	[108]

multimodal ligand on adsorbent is able to interact with proteins through various intermolecular forces to get a high binding capacity in high ionic strength and salt concentration feedstocks [90,92,109–111].

Figures 1.1a and b shows the effects of salt concentrations in buffer on bovine serum albumin (BSA) adsorption isotherms on Streamline DEAE and on Streamline Direct CST I materials, respectively, where Streamline DEAE and Streamline Direct CST I were purchased from Amersham Pharmacia Biotech (now GE Healthcare). Streamline DEAE is a weak anion exchanger with $-O-CH_2CH_2-N^+(C_2H_5)_2H$ functional group, with the following characteristics: its matrix consists of macroporous cross-linked 6% agarose constraining crystalline quartz core materials, with a particle density of 1200 kg m^{-3}, a particle size distribution of 100–300 μm, and a mean particle size of 200 μm. Streamline Direct CST I is an ion exchanger with multimodal functional group, with the

Table 1.3 Suppliers of commercial adsorbents.

Manufacturers	Adsorbent		Matrix
GE Healthcare	Streamline Series	Q XL	6% Cross-linked agarose containing a quartz core with dextran surface extended.
		XL	
		DEAE	6% Cross-linked agarose containing a quartz core.
		SP	
		Phenyl	
		Quartz Base Matrix	
		Heparin	
		Chelating	
		rProtein A	4% Highly cross-linked agarose containing a quartz core.
		Direct CST I	4% Cross-linked agarose containing stainless steel core material.
		Direct HST	Cross-linked agarose containing small stainless steel particles with multi-modal functional groups.
	Sepharose Fast Flow Series		6% Cross-linked agarose without core. The polysaccharide chains arranged in bundles with different degree of intra-chain cross-linking provide high matrix rigidity.
UpFront Chromatography A/S	UFC		6% Cross-linked agarose containing a glass core.
DSM Biologics	Rhobust Fastline Series		Cross-linked agarose containing a Tungsten Carbide core.
	MabDirect Protein A/MM		
Pall BioSepra Corporation	DEAE – Spherodex LS		The porous silica matrix is coated with a continuous layer of ionizable dextran to yield high exchange capacity and improved stability.
	DEAE – Spherodex M		
	CM/S/Q/DEAE – Ceramic HyperD F		Hydrogel polymer with porous ceramic beads.
	Lysine HyperD		Hydrogel polymer within the large pores of rigid beads.
	Heparin HyperD M		Porous rigid mineral bead containing heparin bound, hydrogel filled pores.
	Q/CM HyperZ		Hydrogel-filled porous with zirconium oxide particles.
The Dow Chemical Company	Amberlite XAD7HP		Macroporous acrylic polymer.
Others	Macrosorb K4AX		4% Cross-linked agarose with Kieselguhr particles.

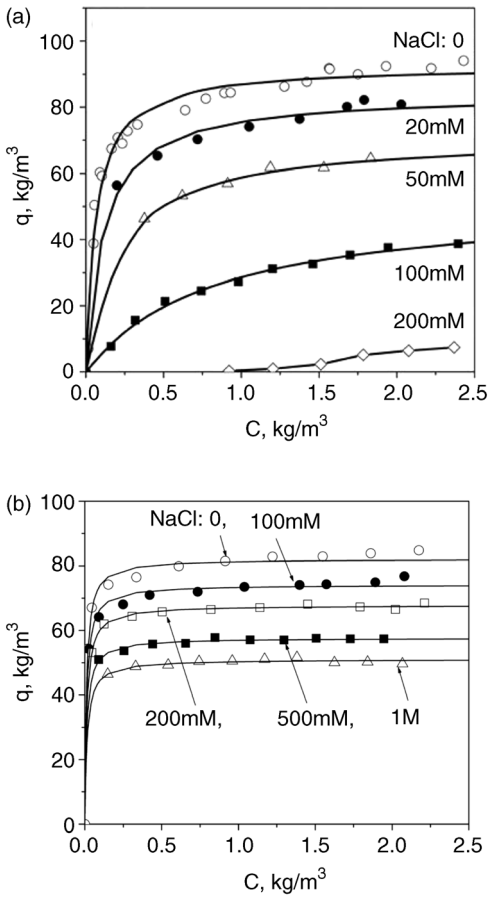

Figure 1.1 Effect of salt concentration in buffer on BSA adsorption isotherms on Streamline DEAE. (a) (20 mM phosphate buffer, pH = 7.5) and on Streamline Direct CST I. (b) (50 mM acetate buffer, pH = 5). Circle points: experimental data. Reprinted from Ref. [90] with permission from John Wiley & Sons.

following characteristics: its matrix consists of macroporous cross-linked 4% agarose constraining stainless steel core materials, with a particle density of 1800 kg m^{-3}, a particle size distribution of 80–165 μm, and a mean particle size of 135 μm.

As shown in Figure 1.1a, the ligand of Streamline DEAE is very sensitive to salt concentration in buffer, so BSA adsorbed on Streamline DEAE can be eluted easily by increasing the salt concentration to 0.5 M in 20 mM phosphate buffer, pH = 7.5. Streamline Direct CST I has a multimodal ligand that is less sensitive to the salt concentration, as shown in Figure 1.1b. Therefore, it is very difficult to elute BSA from Streamline CST I in the column only by increasing the salt

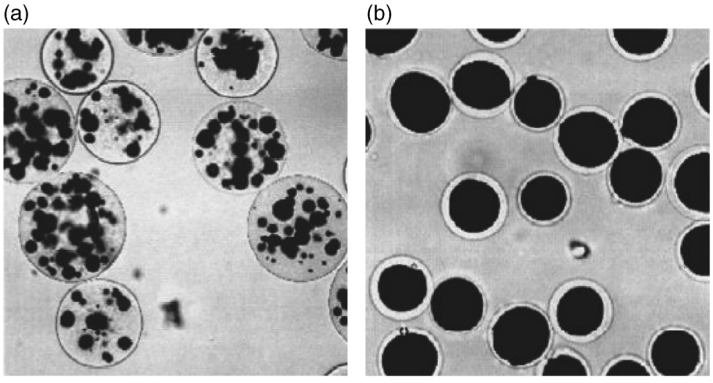

Figure 1.2 Adsorbents with a high-density matrix used in expanded bed. (a) Streamline DEAE/Streamline Direct CST I. (b) Pellicular adsorbent/inert core adsorbent.

concentration in 50 mM acetate buffer, pH = 5. Therefore, to accomplish elution of adsorbed BSA proteins, both salt concentration and pH value in acetate buffer are increased.

In an expanded bed, adsorbents with a high-density matrix are used to form a stable expansion. Recently, some authors have improved the design of the high-density matrix of adsorbent, by including a single heavier inert core material in the macroporous resin matrix, which is called pellicular adsorbent or inert core adsorbent, as shown in Figure 1.2 [30,44]. The inert core adsorbents not only increase the particle density to form stable expansion at high feed flow rate, but also reduce the protein diffusion resistance inside the adsorbent due to shortening of the diffusion path, which made the adsorption behavior in EBA process more efficient.

Usually, the column efficiency is expressed by the theoretical plate number and the height equivalent to a theoretical plate (HETP). HETP is the sum of the independent contributions of liquid axial dispersion, film mass transfer resistance, pore diffusion resistance, and the restricted adsorption–desorption rate. Based on our works [12,49,90,112,113], the theoretical analysis on HETP* is given in Equation 1.1, to demonstrate the potential application of the inert core adsorbents in the fast, high-performance liquid chromatography (HPLC) for the resolution of biological macromolecules as a result of the decrease of the intraparticle diffusion resistance.

$$\mathrm{HETP}^{*} = \frac{2\upsilon(1-\xi_C^3)}{[1+\upsilon(1-\xi_C^3)(1-\xi_C)]^2}\left(\frac{\varepsilon_S u R^2}{\varepsilon_B L}\right) \left[\frac{(1-\xi_C)^2(1-\xi_C)^3}{3}\left(\frac{1}{\Theta}\frac{1}{\varepsilon_S D_P}+\frac{1}{k_f R}\right)+\frac{\xi_m^2}{R^2}\frac{1}{k_{ads}}\right]+\frac{2\varepsilon_B D_L}{uL} \tag{1.1}$$

It is found that the decrease of the intraparticle diffusion resistance by inert core adsorbents is quantitatively estimated by the parameter $1/\Theta$ as

$$\frac{1}{\Theta} = \frac{(1-\xi_C)^2}{\left(1-\xi_C{}^3\right)}\left[\xi_C + \frac{(1-\xi_C)^3}{5\left(1-\xi_C{}^3\right)}\right] \tag{1.2}$$

For conventional adsorbent ($\xi_C = 0$), $1/\Theta = 0.2$; with the increase of ξ_C, the value of $1/\Theta$ drops quickly.

Based on this discussion, we conclude that the efficiency of a chromatographic column packed with inert core adsorbent can be enhanced, especially for systems where the intraparticle diffusion rate is slow. This is the case of biological macromolecules separation by liquid chromatography where biomacromolecules slowly diffuse in the adsorbent pores, including the case of the expanded bed chromatography.

1.2.2
Expanded Bed Adsorption/Desorption of Protein

Expanded bed adsorption technology has been widely applied to capture proteins directly from crude feedstocks, and various applications have been reported from laboratory-scale to pilot-plant and large-scale production [1–8].

In our laboratory, experiments were carried out for the whole expanded bed BSA protein adsorption process with Streamline Direct CST I (Figure 1.3) and with Streamline DEAE (Figure 1.4), where a Streamline 50 column is packed either with Streamline Direct CST I or Streamline DEAE with the same amount of the adsorbents (300 ml). With the same degree of expansion (twice settled bed height), 2 kg m^{-3} BSA aqueous solution is applied to the expanded beds and BSA protein is adsorbed; after the adsorption stage, the bed is washed and BSA protein recovery processes at the elution stage. With Streamline Direct CST I, the

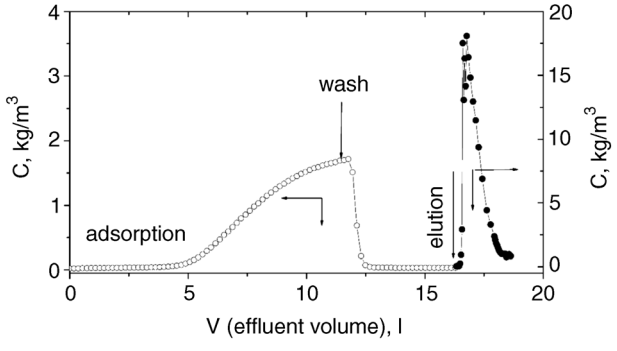

Figure 1.3 Effluent curves of BSA protein during adsorption, washing, and elution stages in expanded bed packed with Streamline Direct CST I. Reprinted from Ref. [90] with permission from John Wiley & Sons, Inc.

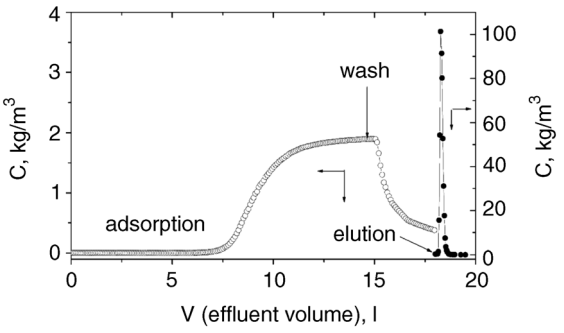

Figure 1.4 Effluent curves of BSA protein during adsorption, washing, and elution stages in expanded bed packed with Streamline DEAE. Reprinted from Ref. [90] with permission from John Wiley & Sons.

operating conditions are as follows: at the adsorption stage, 2 kg m^{-3} BSA aqueous solution, prepared with 50 mM acetate buffer, pH = 5, is applied from the bottom of the expanded bed at 181 ml min^{-1} flow rate; at the washing stage, 50 mM acetate buffer, pH = 5, is applied from the bottom of the expanded bed; and at the elution stage, 50 mM acetate buffer with 1 M NaCl, pH = 7, is applied from the top of the settled bed at 39 ml min^{-1}. With Streamline DEAE, the operating conditions are as follows: at adsorption stage, 2 kg m^{-3} BSA aqueous solution, prepared with 20 mM phosphate buffer, pH = 7.5, is applied from the bottom of the expanded bed at 83.6 ml min^{-1} flow rate; at washing stage, 20 mM phosphate buffer, pH = 7.5, is applied from the bottom of the expanded bed; and at the elution stage, 20 mM phosphate buffer with 0.5 M NaCl, pH = 7.5, is applied from the top of the settled bed at 37 ml min^{-1}.

Based on the experimental results, the comprehensive evaluation of the hydrodynamics, BSA dynamic adsorption capacity, and BSA recovery in the expanded bed adsorption process with Streamline DEAE and with Streamline Direct CST I are summarized as follows:

1) For the same degree of expansion and the same expanded bed height, the high-density Streamline Direct CST I allows a higher feed flow velocity (553 cm h^{-1}) to pass through the expanded bed; in contrast, a low feed flow velocity (259 cm h^{-1}) is allowed to pass through the expanded bed packed with low-density Streamline DEAE.
2) At 5% BSA breakthrough point during expanded bed adsorption, BSA dynamic binding capacity on Streamline Direct CST I is 34 mg (BSA) ml^{-1} of settled bed volume (50 mM buffer) and BSA dynamic binding capacity on Streamline DEAE is 50 mg (BSA) ml^{-1} of settled bed volume (20 mM buffer). However, BSA binding capacity on Streamline Direct CST I is not sensitive to ionic strength in feedstock, which means there is no need for dilution of feedstock arising from high ionic strength. In contrast, BSA binding capacity on Streamline DEAE is very sensitive to the ionic strength

in feedstock; when the ionic strength in feedstock is increased to 50 mM, the BSA adsorption capacity decreases by half.

3) At the washing stage, it is found that BSA effluent concentration quickly drops and approaches the baseline for the expanded bed of Streamline Direct CST I, which means almost irreversible adsorption for BSA binding to Streamline CST I. BSA adsorption on Streamline DEAE is reversible; when washing, some BSA can be desorbed from Streamline DEAE so that the effluent concentration approaches a relatively stable value.
4) The ligand of Streamline DEAE is very sensitive to salt concentration in buffer, so BSA adsorbed on Streamline DEAE can be eluted easily by increasing the salt concentration to 0.5 M in 20 mM phosphate buffer, pH = 7.5. BSA recovery in the whole expanded bed adsorption process reaches 91%. Streamline Direct CST I has a multimodal ligand that is less sensitive to the salt concentration, so it is very difficult to elute BSA from Streamline CST I in the column only by increasing the salt concentration in 50 mM acetate buffer, pH = 5. To accomplish elution of adsorbed BSA proteins, both salt concentration and pH value in acetate buffer are increased. Here, when the elution buffer is 50 mM acetate buffer with 1 M NaCl at pH = 7, BSA recovery attains 87%.

In practical applications, various proteins in source materials prepared from an upstream process or prepared from biological raw materials can be present. When the target protein is captured from these crude feedstocks by an EBA process, the other proteins also competitively bind to adsorbents with the target protein. Therefore, it will be more significant to research multicomponent protein competitive adsorption in an EBA process.

An experiment was carried out to capture both BSA and myoglobin from feedstock by an EBA process, where a Streamline 50 column was packed with 300 ml of Streamline Direct CST I. The feedstock with a mixture of 1 kg m^{-3} BSA and 0.2 kg m^{-3} myoglobin was applied to the expanded bed at 517 cm h^{-1} flow velocity. The expansion degree was about twice settled bed height (30.3/15.3 cm). BSA and myoglobin are adsorbed by suspended Streamline Direct CST I adsorbent in an expanded bed. After the adsorption stage, the bed is washed and the bound BSA and myoglobin are desorbed at the elution stage. The detailed operation procedures have been previously described. The experimental results are shown in Figure 1.5, where circle points represent BSA and triangle points represent myoglobin. The operating conditions are as follows: at the adsorption stage, the feedstock with 1 kg m^{-3} BSA and 0.2 kg m^{-3} myoglobin, prepared with 50 mM acetate buffer (pH 5), is applied from the bottom of the expanded bed at 169 ml min^{-1} flow rate; at the wash stage, 50 mM acetate buffer with pH 5, is applied from the bottom of the expanded bed at about 169 ml min^{-1} flow rate; and at the elution stage, 50 mM phosphate buffer with 1 M NaCl, (pH 7) is applied from the top of the settled bed at 44 ml min^{-1}.

At the binding condition with 50 mM acetate buffer (pH 5), Streamline Direct CST I can efficiently capture both BSA and myoglobin from the feedstock in the

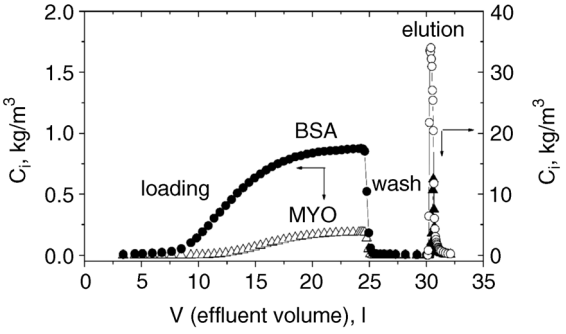

Figure 1.5 Effluent curves of BSA and myoglobin during adsorption, wash and elution stages in expanded bed packed with Streamline Direct CST I. Reprinted from Ref. [92] with permission from John Wiley & Sons, Inc.

expanded bed. At the breakthrough point of 5% BSA feed concentration, BSA dynamic binding capacity is 28.5 mg (BSA) ml^{-1} of settled bed volume, and myoglobin dynamic binding capacity is 5.65 mg (myoglobin) ml^{-1} of settled bed volume. At the washing stage, 50 mM acetate buffer (pH 5) is used to wash the column. It is found that the effluent concentrations both of BSA and myoglobin quickly drop and approach the baseline in an expanded bed of Streamline Direct CST I, which means almost irreversible adsorption of both BSA and myoglobin on Streamline Direct CST I. When the elution buffer, 50 mM phosphate buffer with 1 M NaCl (pH 7), is used in the elution stage, BSA recovery in the whole EBA process can reach 95% and myoglobin recovery reaches 88%, and the consumption amount of the elution buffer is very small, as shown in Figure 1.5.

1.2.3
Modeling of the Expanded Bed

The hydrodynamics and adsorption kinetics in expanded beds are more complex than in fixed beds. The liquid axial dispersion in expanded beds is more significant than in fixed beds; because of the fluidized nature of the expanded bed, adsorbent particle axial dispersion occurs. Moreover, there are variations of particle size axial distribution and bed voidage axial variation in expanded beds for the specially designed adsorbents with wide particle size distribution [78,83,87,114]. Models available for fixed beds may be not adequate to describe the hydrodynamic and adsorption behavior in expanded beds.

Wright and Glasser [80] developed a mathematical model to predict the breakthrough curve for protein adsorption in a fluidized bed, where intraparticle diffusion resistance, film mass transfer resistance, liquid axial dispersion, and adsorbent particle axial dispersion were taken into account. Later, Tong *et al.* [47] and Chen *et al.* [115] used this model to predict the breakthrough curves in the expanded bed adsorption. When capturing proteins in an expanded

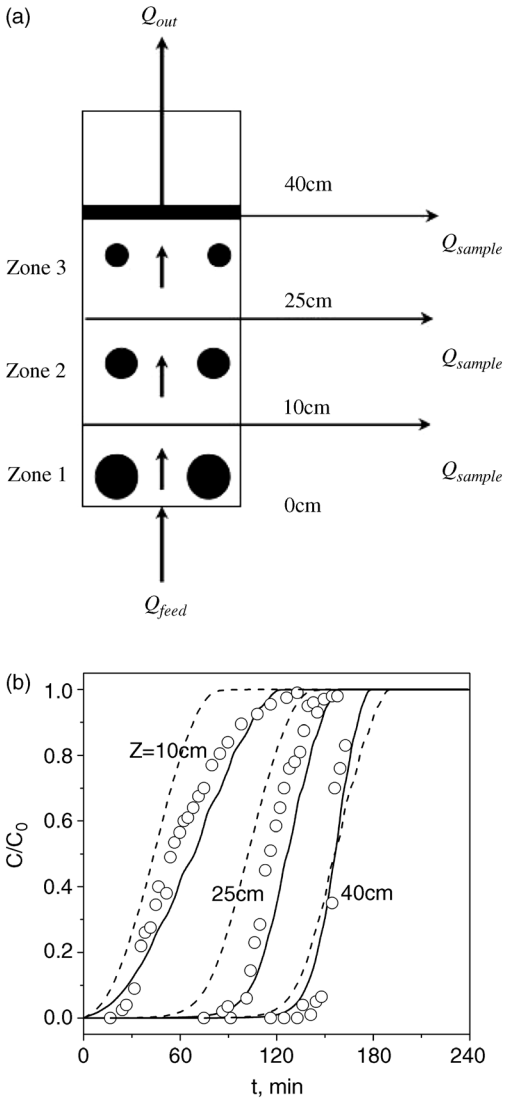

Figure 1.6 (a) Expanded bed with three-zones in Bruce and Chase experimental system (2001) $Q_{feed} = 60.2\ mL \cdot min^{-1}$; $Q_{out} = 58.9\ mL \cdot min^{-1}$, and $Q_{sample} = 1.3/3.0\ mL \cdot min^{-1}$ (b) Comparison among the in-bed experimental breakthrough curves and the simulation results. Circle points: experimental data [83]; solid lines: simulation results with three-zone model; dashed lines: simulation results with uniform model. Reprinted from Ref. [13] with permission from Elsevier.

bed with a high flow velocity, the slow diffusion rate of proteins results in high intraparticle diffusion resistance, significantly affecting the breakthrough curve. It is argued that, in this case, the particle size, characterizing the diffusion path in the adsorbent particles, should have a substantial effect on the breakthrough

curves [71]. Therefore, simulation results should be improved when the particle size axial distribution and bed voidage axial variations are taken into account in the model. Tong *et al.* [86] modified the mathematical model by taking into account the particle size axial distribution in expanded beds. Following their experimental research using in-bed monitoring in expanded beds, Bruce and Chase [84] predicted the in-bed breakthrough curves in expanded bed by using zonaly measured parameters. Recently, Kaczmarski and Bellot [116] also made the theoretical investigation about the effects of the axial and local particle size distribution and bed voidage axial variation on the breakthrough curves in expanded beds.

In our laboratory, a three-zone model was developed [13] to predict in-bed breakthrough curves and confirmed the effect of the particle size axial distribution and bed voidage axial variation on the breakthrough curves in expanded beds. In expanded beds, the adsorbent particle size, bed voidage, and liquid axial dispersion coefficient are very different at the bottom zone, the middle zone, and the top zone of the column, and significantly affect the adsorption behavior. The three-zone model, in which the zonal values for these parameters are used, can predict simultaneously in-bed breakthrough curves at the bottom, the middle, and the top of the column. The simulation results by this three-zone model closely fit the experimental data from literature of Bruce and Chase [84], as shown in Figure 1.6. By contrast, the conventional uniform model, in which all the model parameters are estimated by averaged values over the whole column, does not satisfactorily predict in-bed breakthrough curves. When the uniform model is modified by taking into account the bed voidage and the adsorbent particle size axial distribution, the accuracy of the modified uniform model is improved. According to the simulation results, it is found that even for small proteins (i.e., lysozyme), the intraparticle diffusion resistance is also high in expanded bed adsorption. When capturing macromolecular protein at high flow rates in expanded beds, the intraparticle diffusion resistance is expected to be significant. This work supports observations that the use of pellicular and inert core adsorbents can improve the separation performance of proteins in expanded beds due to significant decrease of the intraparticle diffusion resistance by shortening the adsorbent's diffusion path.

1.3
Proteins Separation and Purification by Salt Gradient Ion Exchange SMB

In downstream processing, the frequently used chromatographic methods for separating and purifying proteins take advantage of physical properties that vary from one protein to the other, including size, charge, hydrophobicity, and specially binding capacity. The separation method based on the difference of protein size or shape is called size exclusion (gel filtration) chromatography (SEC). Ion exchange chromatography takes advantage of the charge–charge interaction between protein and ligand, while hydrophobic interaction chromatography

(HIC) or reversed-phase chromatography (RPC) takes advantage of the hydrophobic interaction between protein and ligand, and affinity chromatography (AC) is based on the specific binding between protein and ligand.

Research on the separation and purification of proteins by SMB technology started with size exclusion–simulated moving bed (SE-SMB) chromatography, for its design simplicity in terms of the liquid and solid flow rate ratios (linear distribution coefficients for all proteins on porous stationary phases). In the last decade, it was found that the process performance of the separation and purification of proteins by ion exchange SMB can be improved when a lower salt concentration is formed in sections III and IV to increase the adsorption of proteins and a higher salt concentration is formed in sections I and II to improve the desorption of the bound proteins, called salt gradient ion exchange SMB.

1.3.1 Adsorption Isotherms and Kinetics of BSA and Myoglobin on Ion Exchange Resins

Small molecules, such as small peptides, interact with the ligand on adsorbent by single point attachment, and their migration velocity depends directly on the binding constant of a single bond. Large molecules, such as proteins and nucleic acids, interact with the ligand on adsorbent by multipoint attachment, and their migration velocity depends on the sum of several bonds. Therefore, proteins competitive adsorption on adsorbent is more complex than small molecules. In the published works, Skidmore and Chase [117] investigated the simultaneous adsorption of lysozyme and BSA in a fixed bed packed with the cation exchanger SP-Sepharose-FF; Weinbrenner and Etzel [118] investigated the simultaneous adsorption of BSA and lactalbumin on cation exchange membranes; Martin *et al.* [119] and Lewus and Carta [39] investigated the adsorption of lysozyme/cytochrome C mixtures on the cation exchanger SP-Sepharose-FF and S HyperD-M, respectively; and Hubbuch *et al.* [120] measured the breakthrough curves of an IgG/BSA solution in a fixed bed packed with the cation exchanger SP-Sepharose-FF. These authors reached the same conclusion with regard to the competitive nature of protein binding also leading to a roll up of concentration of the less strongly adsorbed protein in some binding conditions.

In our laboratory [121], ion exchange equilibrium isotherms of BSA and myoglobin on Q-Sepharose FF anion exchanger resin were studied experimentally over a wide protein concentration range, as shown in Figure 1.7. Q-Sepharose FF is a strong anion exchanger with $-CH_2-N^+-(CH_3)_3$ functional group, with the following characteristics: its matrix consists of macroporous cross-linked 6% agarose, a particle size distribution of 45–165 μm, and a mean particle size of 90 μm. From Figure 1.7, BSA has a high ion exchange capacity on Q-Sepharose FF resin at pH 8 Tris buffer (10 mM), with a high favorable nonlinear equilibrium isotherm, as a result of isoelectric point (pI 4.7) of BSA far from buffer pH value (pH 8). The ion exchange equilibrium isotherm of BSA on Q-Sepharose FF resin with the dependence on NaCl concentrations can be represented by the SMA model as follows:

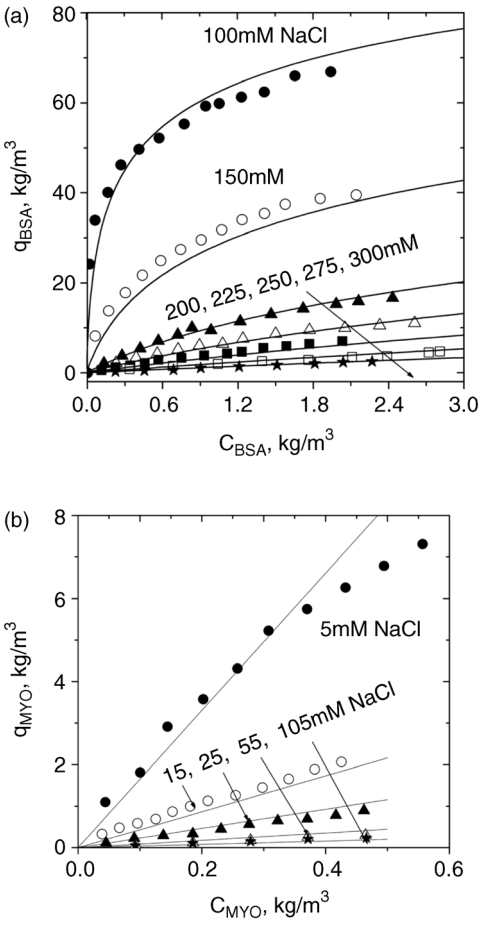

Figure 1.7 Ion exchange equilibrium isotherms of (a) BSA and (b) myoglobin on Q-Sepharose FF resin at room temperature (~25 °C), in 10 mM Tris buffer (pH 8). Points: experimental data; lines: calculated by Equation 1.3 for BSA, by Equation 1.4 for myoglobin. Reprinted from Ref. [121] with permission from John Wiley & Sons, Inc.

$$C_{\mathrm{BSA}} = \frac{q_{\mathrm{BSA}}^{\mathrm{IE}} C_{\mathrm{S}}^{Z_{\mathrm{BSA}}}}{K_{\mathrm{BSA}}[q_0 - (Z_{\mathrm{BSA}} + \sigma_{\mathrm{BSA}}) q_{\mathrm{BSA}}^{\mathrm{IE}} / M_{\mathrm{BSA}}]^{Z_{\mathrm{BSA}}}} = \frac{q_{\mathrm{BSA}}^{\mathrm{IE}} C_{\mathrm{S}}^{6.03}}{10.83[0.210 - (6.03 + 75) q_{\mathrm{BSA}}^{\mathrm{IE}} / M_{\mathrm{BSA}}]^{6.03}} \tag{1.3}$$

Since pH value (pH 8) in 10 mM Tris buffer approaches the isoelectric point of myoglobin (pI 7.4), the ion exchange amount of myoglobin on Q-Sepharose FF resin is very small even at lower salt concentrations. Over a wide myoglobin concentration range, linear ion exchange equilibrium isotherms can be found at

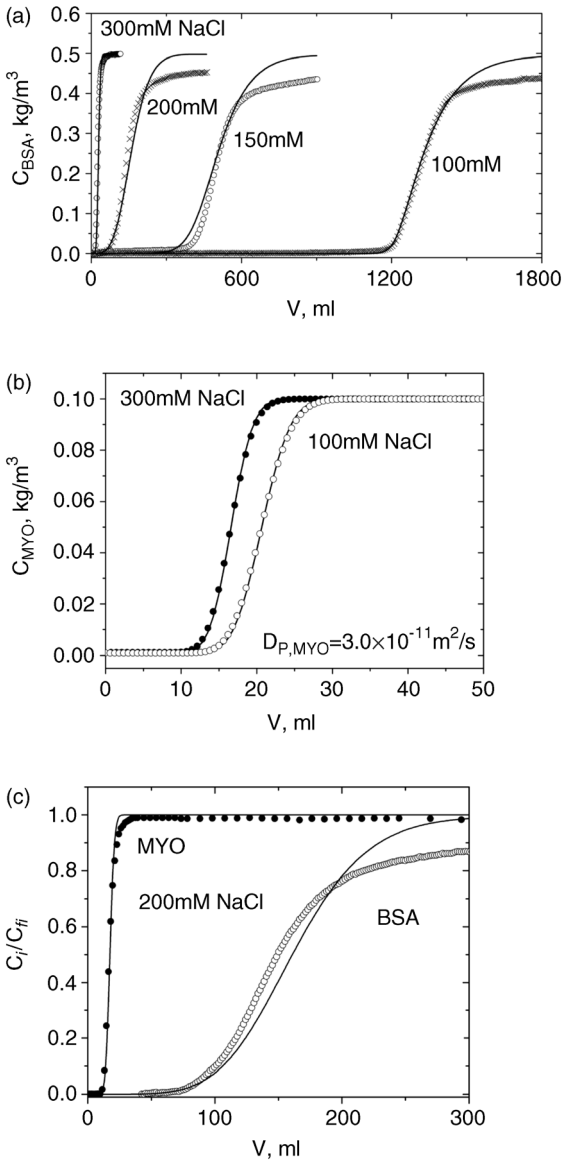

Figure 1.8 BSA and myoglobin breakthrough curves at various NaCl concentrations. Circle points: experimental data; lines: simulation results with LDF model. (a) BSA; (b) myoglobin; (c) BSA and myoglobin competitive adsorption. Reprinted from Ref. [121] with permission from John Wiley & Sons, Inc.

various NaCl concentrations. Based on the experimental results shown in Figure 1.7b, the linear ion exchange equilibrium isotherm of myoglobin on Q-Sepharous FF resin is expressed as follows:

$$q_{\mathrm{MYO}}^{\mathrm{IE}} = \frac{K_{\mathrm{MYO}} q_0^{Z_{\mathrm{MYO}}}}{C_{\mathrm{S}}^{Z_{\mathrm{MYO}}}} C_{\mathrm{MYO}} = 0.02576\, C_{\mathrm{S}}^{-1.22} C_{\mathrm{MYO}} \tag{1.4}$$

Furthermore, breakthrough curves of BSA and myoglobin are measured in a fixed bed, as shown in Figure 1.8a–c, where a XK16/20 column is packed with Q-Sepharous FF anion exchangers, packed height of 100 mm, column diameter of 16 mm, and bed voidage of 0.35. The experimental breakthrough curves are compared with the simulation results, as shown in Figure 1.8, to confirm the accuracy of ion exchange equilibrium isotherm expressions (Equation 1.3 for BSA and Equation 1.4 for myoglobin). The diffusion coefficients of BSA and myoglobin are evaluated by fitting the experimental data of breakthrough curves with LDF model, as $D_{\mathrm{Pe,BSA}} = 1.5 \times 10^{-11}\mathrm{m^2\,s^{-1}}$ and $D_{\mathrm{Pe,MYO}} = 3.0 \times 10^{-11}\mathrm{m^2\,s^{-1}}$, respectively.

In ion exchange chromatography, the separation factor of proteins depends evidently on salt concentration. Table 1.4 lists the separation factors of BSA to myoglobin by Q-Sepharose FF anion exchanger at various salt concentrations; here, separation factor is defined as $S_{1,2} = (q_1/C_1)/(q_2/C_2)$.

With a low NaCl concentration in Tris buffer (pH 8), the separation factor of BSA to myoglobin is large; for example, with 200 mM NaCl, $S_{\mathrm{BSA,MYO}}$ goes up to 18.23, BSA and myoglobin can be separated easily by ion exchange chromatography. With the increase of salt concentration, the separation factor decreases. When salt concentration is 400 mM NaCl, the separation factor approaches unity, which means BSA and myoglobin cannot be separated by ion exchange chromatography. This phenomenon is called azeotrope [17–19], like azeotropic

Table 1.4 Separation factor of BSA to myoglobin by Q-Sepharose FF anion exchanger under linear adsorption equilibrium isotherm.

Salt concentration in 10 mM Tris buffer (pH 8)	K_{BSA}	K_{MYO}	$S_{\mathrm{BSA,MYO}}$	Comments
200 mM NaCl	15.02	0.82	18.23	BSA: the more retained Myoglobin: the less retained
250 mM NaCl	4.28	0.78	5.48	BSA: the more retained Myoglobin: the less retained
300 mM NaCl	1.75	0.75	2.33	BSA: the more retained Myoglobin: the less retained
350 mM NaCl	0.99	0.73	1.35	BSA: the more retained Myoglobin: the less retained
400 mM NaCl	0.71	0.72	0.99	Azeotrope
500 mM NaCl	0.55	0.70	0.78	Myoglobin: the more retained BSA: the less retained Similar to size exclusion SMB

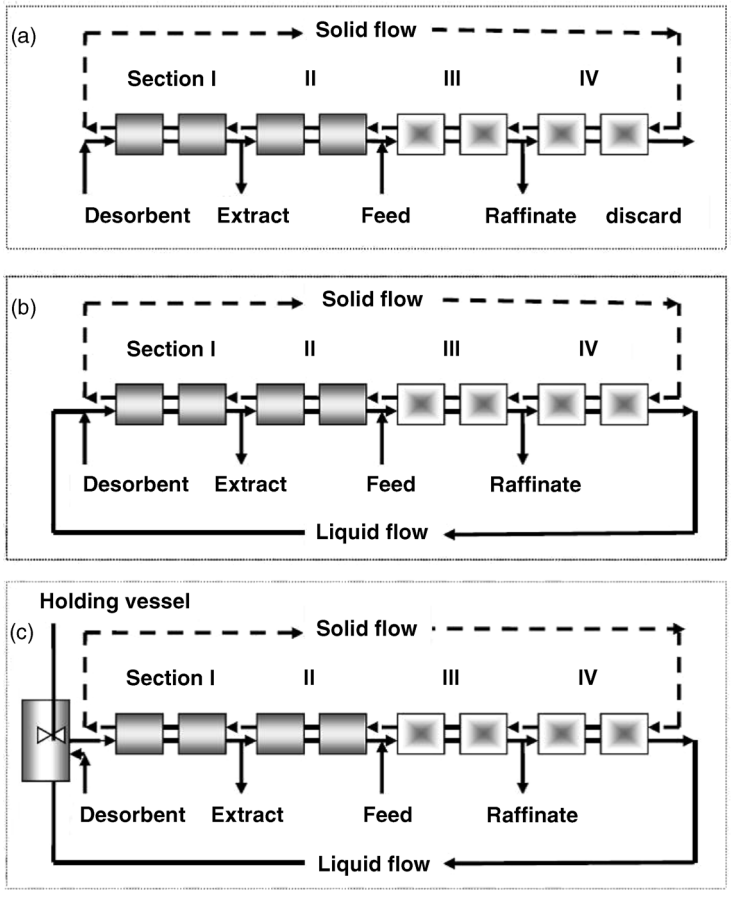

Figure 1.9 Operation modes for gradient IE-SMB: (a) gradient IE-SMB with open loop; (b) gradient IE-SMB with closed loop; (c) gradient IE-SMB with closed loop and a holding vessel. ▭: higher solvent strength; ▭: lower solvent strength. Reprinted from Ref. [121] with permission from John Wiley & Sons, Inc.

distillation. Further increasing salt concentration, it will be found a reversal of separation since myoglobin becomes the more retained component and BSA becomes the less retained component, and the separation behavior of BSA and myoglobin in ion exchange chromatography is more close to that in size exclusion chromatography.

1.3.2
Salt Gradient Formation and Process Design for IE-SMB Chromatography

It is well known that the binding capacity of the classical ion exchanger to proteins is sensitive to salt concentration in the feedstock; the higher the salt

concentration is, the lower the binding capacity to the proteins is. Therefore, a stepwise gradient can be formed by introducing a lower salt concentration at the feed port compared to a higher salt concentration introduced at the desorbent port; then the ion exchanger has a lower binding capacity for proteins in sections I and II to improve the desorption and has a stronger binding capacity in sections III and IV to increase adsorption in the IE-SMB chromatography.

In the separation and purification of proteins by SMB chromatography, the open loop configuration was used by many authors in order to avoid the accumulation of contaminants in the columns, as shown in Figure 1.9a, where the liquid stream from section IV is discarded, instead of being recycled to the desorbent stream for further reduction of desorbent consumption. It is well known that one advantage of SMB chromatography compared with fixed bed chromatography is the reduced desorbent consumption. This can be achieved in the closed loop configuration by recycling the liquid stream from section IV to the desorbent inlet of section I, as shown in Figure 1.9b, which is very important for Reverse phase simulated moving bed RP-SMB chromatography. However, in gradient SMB chromatography, the recycling of liquid stream is more complicated. The solvent strength in the eluent is different in sections I and IV, and the effluent composition from section IV varies in a dynamic manner during a switch time interval. This complicates the direct recycling of the eluent [122]. In Figure 1.9c, a holding vessel with a given volume is added to the system to mix the desorbent with the recycled liquid stream from section IV during a switch time interval, in order to reduce the fluctuation of the solvent strength in the columns, as shown in Figure 1.10.

1.3.3
Separation Region of Salt Gradient IE-SMB Chromatography

With a stable stepwise salt gradient IE-SMB chromatography, if one wants to recover the less retained protein (myoglobin) from the raffinate stream and the more retained protein (BSA) from extract stream with a high purity, some constraints have to be met. These constraints are expressed in terms of the net fluxes of proteins in each section: BSA must move upward in section I, myoglobin must move upward while the net flux of BSA must be downward in sections II and III, and the net flux of myoglobin has to be downward in section IV. Table 1.5 summarizes these constraint conditions to the net fluxes for the separation of BSA and myoglobin in salt gradient IE-SMB chromatography.

The operating conditions given in Table 1.5 are only necessary and not sufficient. Usually, a separation region is used for the selection of the optimum flow rate in each section of SMB unit. The separation region is the area in a $\gamma_2 \times \gamma_3$ plot where both extract and raffinate are pure. This plot [123], is an important tool in the choice of the best operating conditions, provided that the constraints in sections I and IV are fulfilled, that is, the flow rate ratios in sections I and IV are far from its constraint values. When resistances to mass transfer are

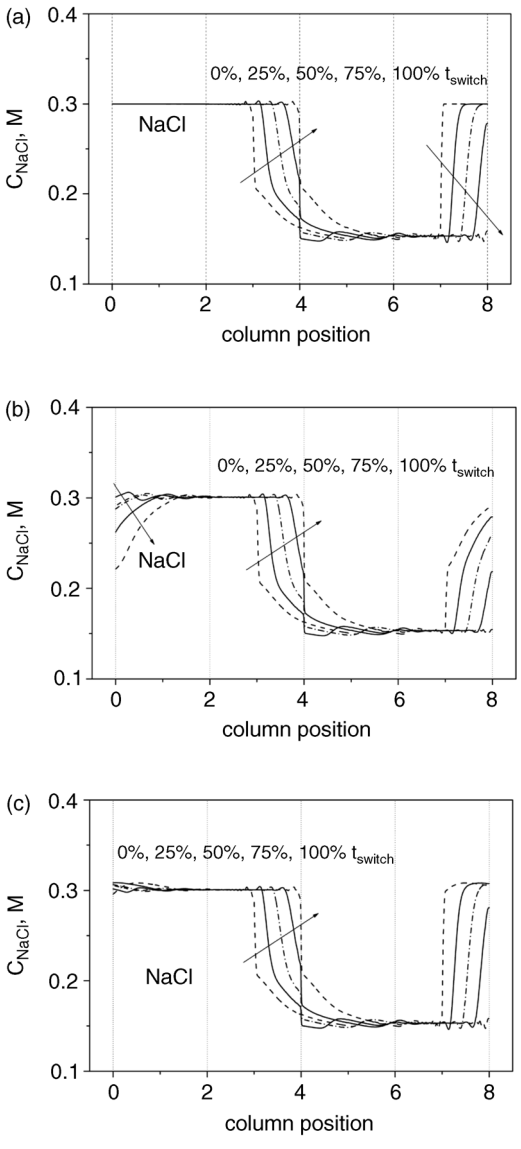

Figure 1.10 Salt gradient formations in IE-SMB chromatography with (a) open loop, (b) closed loop, and (c) closed loop with a holding vessel ($V_s = 10$ ml). Reprinted from Ref. [121] with permission from John Wiley & Sons.

significant, the separation region will shrink, especially for the macromolecular bioseparation where the intraparticle diffusion resistance is more important [124–126]. Here, γ_j are the ratios between the net fluid and solid interstitial velocities, and are related to the m_j ratios used by Morbidelli and coworkers by

Table 1.5 Some constraints to the net fluxes for BSA and myoglobin separation in salt gradient ion exchange SMB.

	Salt	BSA	Myoglobin
Section I	$\frac{Q_{\mathrm{I}}^{\mathrm{TMB}}}{Q_{\mathrm{S}}}\frac{C_{\mathrm{SI}}}{q_{\mathrm{SI}}} > 1$	$\frac{Q_{\mathrm{I}}^{\mathrm{TMB}}}{Q_{\mathrm{S}}}\frac{C_{\mathrm{BSAI}}}{q_{\mathrm{BSAI}}} > 1$	
Section II	$\frac{Q_{\mathrm{II}}^{\mathrm{TMB}}}{Q_{\mathrm{S}}}\frac{C_{\mathrm{SII}}}{q_{\mathrm{SII}}} > 1$	$\frac{Q_{\mathrm{II}}^{\mathrm{TMB}}}{Q_{\mathrm{S}}}\frac{C_{\mathrm{BSAII}}}{q_{\mathrm{BSAII}}} < 1$	$\frac{Q_{\mathrm{II}}^{\mathrm{TMB}}}{Q_{\mathrm{S}}}\frac{C_{\mathrm{MYOII}}}{q_{\mathrm{MYOII}}} > 1$
Section III	$\frac{Q_{\mathrm{III}}^{\mathrm{TMB}}}{Q_{\mathrm{S}}}\frac{C_{\mathrm{SIII}}}{q_{\mathrm{SIII}}} > 1$	$\frac{Q_{\mathrm{III}}^{\mathrm{TMB}}}{Q_{\mathrm{S}}}\frac{C_{\mathrm{BSAIII}}}{q_{\mathrm{BSAIII}}} < 1$	$\frac{Q_{\mathrm{III}}^{\mathrm{TMB}}}{Q_{\mathrm{S}}}\frac{C_{\mathrm{MYOIII}}}{q_{\mathrm{MYOIII}}} > 1$
Section IV	$\frac{Q_{\mathrm{IV}}^{\mathrm{TMB}}}{Q_{\mathrm{S}}}\frac{C_{\mathrm{SIV}}}{q_{\mathrm{SIV}}} > 1$		$\frac{Q_{\mathrm{IV}}^{\mathrm{TMB}}}{Q_{\mathrm{S}}}\frac{C_{\mathrm{MYOIV}}}{q_{\mathrm{MYOIV}}} < 1$

$$\gamma_j = \frac{\nu_j^{\mathrm{TMB}}}{u_{\mathrm{S}}} = \frac{1-\varepsilon_{\mathrm{B}}}{\varepsilon_{\mathrm{B}}} m_j \tag{1.5}$$

And

$$m_j = \frac{Q_j^{\mathrm{TMB}}}{Q_{\mathrm{S}}} = \frac{Q_j^{\mathrm{TMB}} - Q_{\mathrm{S}}\varepsilon_{\mathrm{B}}/(1-\varepsilon_{\mathrm{B}})}{Q_{\mathrm{S}}} \tag{1.6}$$

In this work, the separation regions are evaluated by the gradient SMB model where both mass transfer resistance in particles and axial liquid dispersion in columns are taken into account, as shown in Figure 1.11. In this figure, three separation regions are demonstrated for the separation of BSA and myoglobin by salt gradient IE-SMB with open loop configuration under nonlinear adsorption equilibrium isotherm. The configuration of the IE-SMB unit and operating

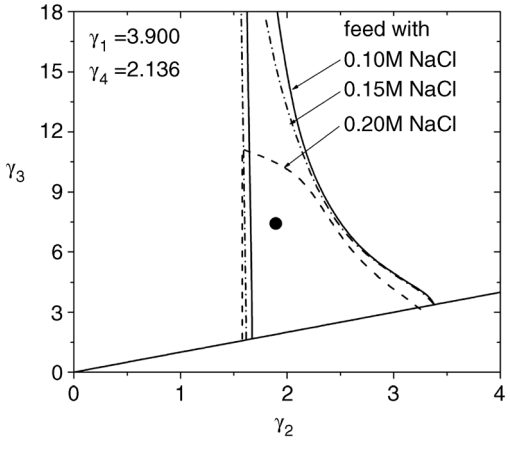

Figure 1.11 Separation regions for BSA and myoglobin separation by salt gradient IE-SMB with open loop at nonlinear adsorption isotherm. Circle point: operating conditions for the calculations in Figure 1.12. Reprinted from Ref. [127] with permission from Taylor & Francis.

conditions for calculations are listed in the published paper by Li *et al.* [121], γ_1 and γ_4 are assigned to be 3.900 and 2.136; and protein purities are imposed to be above 99% for both raffinate and extract streams for the design of the separation region. During the simulations, the NaCl concentration in desorbent is constant and equal to 0.3 M, while the NaCl concentration in the feedstock is assigned to be 0.1, 0.15, and 0.2 M, respectively.

Based on the simulation results shown in Figure 1.11, the effect of the salt concentration in feed on the separation region is significant, and the separation region shrinks with the increase of the salt concentration in feedstock (0.1, 0.15, and 0.2 M NaCl, respectively) if the NaCl concentration in desorbent is constant and equal to 0.3 M. The range of the allowable flow rate in section II (γ_2) is narrower as a result of the higher NaCl concentration formed in sections I and II and resins having a small separation factor to the separation of BSA and myoglobin. The range of the allowable flow rate in section III (γ_3) is broader as a result of the lower NaCl concentration formed in sections III and IV and resins having a big separation factor; moreover, the lower the NaCl concentration formed in sections III and IV, the broader the range of the allowable flow rate in section III, as shown in Figure 1.11 for the cases formed by the feedstock with 0.1, 0.15, and 0.2 M NaCl, respectively. When the feed has a lower NaCl concentration, such as 0.1 or 0.15 M, the BSA adsorption capacity on Q-Sepharous FF resin is very high, the maximum allowable flow rate in section III (γ_3) will probably be restricted either by the pressure drop limitation or by the re-equilibrium (the sufficient retention time) for proteins and salt, instead of being limited by the adsorption equilibrium isotherm of BSA, which is very different from that for the resolution of similar products with a small separation factor. In addition, for our model system (BSA/myoglobin separation by Q-Sepharose FF resin) the minimum flow rate in section II is restricted by the salt upward movement, instead of being limited by the myoglobin adsorption equilibrium isotherm, in order to obtain a stable salt gradient in the IE-SMB unit.

1.3.4
Proteins Separation and Purification in Salt Gradient IE-SMB with Open Loop Configuration

Figure 1.12 shows the typical concentration profiles of BSA, myoglobin, and NaCl in the salt gradient IE-SMB chromatography, where the actual operating condition is selected inside the separation region for the case of the feed with 0.15 M NaCl (represented as a circle point in Figure 1.11). With the setup salt gradient in IE-SMB unit packed with Q-Sepharose FF resins, BSA is recovered completely from the extract stream with 2.76 enrichment of BSA concentration to that of the feed, while myoglobin is eluted both from the raffinate stream and from the section IV exit in the open loop SMB unit. The practical example is that binary separation of proteins with the requirement of complete recovery from extract stream and from raffinate stream in salt gradient SMB chromatography with open loop configuration, for our separation system, which is BSA

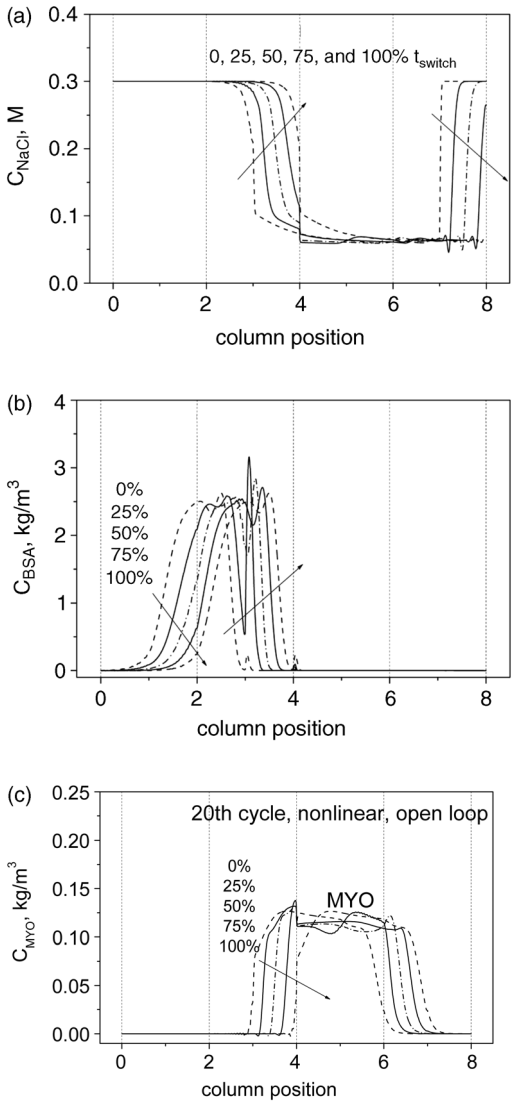

Figure 1.12 Cyclic steady state internal concentration profiles during a switch time interval in salt gradient IE-SMB with open loop when $C_S^F = 0.05$ M NaCl and $C_S^D = 0.3$ M NaCl for BSA and myoglobin separation at nonlinear equilibrium isotherm. Operating conditions as shown by circle point in Figure 1.11. Twentieth cycle, nonlinear, open loop (a) NaCl and (b) BSA (c) MYO. Reprinted from Ref. [127] with permission from Taylor & Francis.

recovered completely from extract stream and myoglobin recovered completely from raffinate stream. For this case, the selection of flow rate in section IV is constrained both by the upward movement of the net flux of salt and the downward movement of the net flux of myoglobin to the raffinate port. As shown in Figure 1.12, a relatively lower salt concentration should be formed in sections III and IV by introducing the feed with 0.05 M NaCl, in order to increase myoglobin ion exchange amount and promote the downward movement of myoglobin in section IV to raffinate port. However, with such a low salt concentration formed in sections III and IV, the other contaminants probably adsorb to the anion exchangers. An alternative method is to adjust the pH value in the buffer to improve the myoglobin ion exchange amount in sections III and IV, such as increasing the pH value in the buffer to 8.5 or 9, in order that a relatively high salt concentration can be used in sections III and IV to prevent the other contaminants from being adsorbed on Q-Sepharose FF resin.

Although an open loop configuration in salt gradient IE-SMB unit is adopted to avoid the accumulation of contaminants in the columns, there exists the possible denaturation or the loss of biological properties of the proteins after a number of cycles of IE-SMB. The buffer compositions, pH value, salt concentration, protein concentration in columns, and flow rate in each section of SMB unit will also affect the bioactivity of the proteins during the actual operation. Therefore, the actual operating conditions for protein separation by salt gradient IE-SMB chromatography should be selected based on the comprehensive considerations of protein purity, recovery, and bioactivity.

1.4 Conclusion

The EBA process will be more effective for those adsorbents that have both high-density base matrix and salt-tolerant ligand. Multimodal functional groups are immobilized on Streamline Direct CST I adsorbents, which not only take advantage of electrostatic interaction, but also take advantage of hydrogen bond interaction and hydrophobic interaction to tightly bind proteins, in order to get a high binding capacity in high ionic strength and salt concentration feedstock. Moreover, the inert core adsorbents not only increase the particle density to form stable expansion at high feed flow rate in the expanded bed, but also reduce the protein diffusion resistance inside the adsorbent due to shortening of the diffusion path. More work is needed when multimodal ligands are immobilized on inert core adsorbents to effectively capture proteins in expanded bed adsorption process.

The process performance of the separation and purification of proteins by ion exchange SMB can be improved when a lower salt concentration is formed in sections III and IV to increase the adsorption of proteins and a higher salt concentration is formed in sections I and II to improve the desorption of the bound proteins, called salt gradient ion exchange SMB. The selection of salt

gradient is a key issue and also is flexible in the design of salt gradient ion exchange SMB chromatography. In sections I and II of ion exchange SMB, a high salt concentration will favor the desorption of the bound proteins and reduce the desorbent consumption, but too high salt concentration should be avoided, as a result of the significant decrease of separation factor in section II; in sections III and IV of ion exchange SMB, a lower salt concentration will favor the adsorption of proteins, but for the case of protein purification from a stream with some impurities, the salt concentration should be raised a little to decrease the adsorption of impurities and contaminants on ion exchangers. Moreover, when the gradient SMB is run in closed loop to reduce further desorbent consumption, it is better that a holding vessel with a given volume is added to the system to mix the desorbent with the recycled liquid stream from section IV in order to reduce salt or solvent strength fluctuation in the columns of section I.

References

1 Chase, H.A. (1994) Purification of proteins by adsorption chromatography in expanded beds. *Trends Biotechnol.*, **12**, 296–303.

2 Hjorth, R. (1997) Expanded bed adsorption in industrial bioprocessing: recent developments. *Trends Biotechnol.*, **15**, 230–235.

3 Thömmes, J., Bader, A., Halfar, M., Karau, A., and Kula, M.R. (1996) Isolation of monoclonal antibodies from cell containing hybridoma broth using a protein A coated adsorbent in expanded beds. *J. Chromatogr. A*, **752**, 111–122.

4 Ujam, L.B., Clemmitt, R.H., Clarke, S.A., Brooks, R.A., Rushton, N., and Chase, H.A. (2003) Isolation of monocytes from human peripheral blood using immuno-affinity expanded-bed adsorption. *Biotechnol. Bioeng.*, **83**, 554–566.

5 Clemmitt, R.H. and Chase, H.A. (2002) Direct recovery of glutathione S-transferase by expanded bed adsorption: anion exchange as an alternative to metal affinity fusions. *Biotechnol. Bioeng.*, **77**, 776–785.

6 Smith, M.P., Bulmer, M.A., Hjorth, R., and Titchener-Hooker, N.J. (2002) Hydrophobic interaction ligand selection and scale-up of an expanded bed separation of an intracellular enzyme from *Saccharomyces cerevisiae*. *J. Chromatogr. A*, **968**, 121–128.

7 Bai, Y. and Glatz, C.E. (2003) Capture of a recombinant protein from unclarified canola extract using Streamline expanded bed anion exchange. *Biotechnol. Bioeng.*, **81**, 855–864.

8 Anspach, F.B., Curbelo, D., Hartmann, R., Garke, G., and Deckwer, W.D. (1999) Expanded-bed chromatography in primary protein purification. *J. Chromatogr. A*, **865**, 129–144.

9 Jahanshahi, M., Sun, Y., Santos, E., Pacek, A., Franco, T.T., Nienow, A., and Lyddiatt, A. (2002) Operational intensification by direct product sequestration from cell disruptates: application of a pellicular adsorbent in a mechanically integrated disruption-fluidised bed adsorption process. *Biotechnol. Bioeng.*, **80**, 201–212.

10 Broughton, D.B. and Gerhold, C.G. (1961) Continuous sorption process employing fixed bed of sorbent and moving inlets and outlets. US Patent 2,985,589.

11 Juza, M., Mazzotti, M., and Morbidelli, M. (2000) Simulated moving-bed chromatography and its application to chirotechnology. *Trends Biotechnol.*, **18** (3), 108–118.

12 Li, P., Xiu, G.H., and Rodrigues, A.E. (2004) Modeling breakthrough and elution curves in fixed bed of inert core adsorbents: analytical and approximate solutions. *Chem. Eng. Sci.*, **59** (15), 3091–3103.

13 Li, P., Xiu, G.H., and Rodrigues, A.E. (2004) A 3-zone model for protein adsorption kinetics in expanded beds. *Chem. Eng. Sci.*, **59** (18), 3837–3847.

14 Ruthven, D.M. and Ching, C.B. (1989) Countercurrent and simulated countercurrent adsorption separation processes. *Chem. Eng. Sci.*, **44** (5), 1011–1038.

15 Gottschlich, N. and Kasche, V. (1997) Purification of monoclonal antibodies by simulated moving-bed chromatography. *J. Chromatogr. A*, **765** (2), 201–206.

16 Imamoglu, S. (2002) Simulated moving bed chromatography (SMB) for application in bioseparation. *Adv. Biochem. Eng. Biotechnol.*, **76**, 211–231.

17 Houwing, J., van Hateren, S.H., Billiet, H. A.H., and van der Wielen, L.A.M. (2002) Effect of salt gradients on the separation of dilute mixtures of proteins by ion-exchange in simulated moving beds. *J. Chromatogr. A*, **952** (1–2), 85–98.

18 Houwing, J., Billiet, H.A.H., and van der Wielen, L.A.M. (2002) Optimization of azeotropic protein separations in gradient and isocratic ion-exchange simulated moving bed chromatography. *J. Chromatogr. A*, **944** (1–2), 189–201.

19 Houwing, J., van Hateren, S.H., Billiet, H.A.H., and van der Wielen, L.A.M. (2002) Effect of salt gradients on the separation of dilute mixtures of proteins by ion-exchange in simulated moving beds. *J. Chromatogr. A*, **952** (1–2), 85–98.

20 Xie, Y., Mun, S., Kim, J., and Wang, N.H. L. (2002) Standing wave design and experimental validation of a tandem simulated moving bed process for insulin purification. *Biotechnol. Prog.*, **18** (6), 1332–1344.

21 Paredes, G., Mazzotti, M., Stadler, J., Makart, S., and Morbidelli, M. (2005) SMB operation for three-fraction separations: purification of plasmid DNA. *Adsorption*, **11**, 841–845.

22 Geisser, A., Hendrich, T., and Boehm, G. (2005) Separation of lactose from human milk oligosaccharides with simulated moving bed chromatography. *J. Chromatogr. A*, **1092** (1), 17–23.

23 Andersson, J. and Mattiasson, B. (2006) Simulated moving bed technology with a simplified approach for protein purification: separation of lactoperoxidase and lactoferrin from whey protein concentrate. *J. Chromatogr. A*, **1107** (1–2), 88–95.

24 Jensen, T.B., Reijns, T.G.P., Billiet, H.A.H., and van der Wielen, L.A.M. (2000) Novel simulated moving bed method for reduced solvent consumption. *J. Chromatogr. A*, **873** (2), 149–162.

25 Antos, D. and Seidel-Morgenstern, A. (2001) Application of gradients in the simulated moving bed process. *Chem. Eng. Sci.*, **56** (23), 6667–6682.

26 Antos, D. and Seidel-Morgenstern, A. (2002) Two-step solvent gradients in simulated moving bed chromatography–numerical study for linear equilibria. *J. Chromatogr. A*, **944** (1–2), 77–91.

27 Abel, S., Mazzotti, M., and Morbidelli, M. (2002) Solvent gradient operation of simulated moving beds. I. Linear isotherms. *J. Chromatogr. A*, **944** (1–2), 23–39.

28 Abel, S., Mazzotti, M., and Morbidelli, M. (2004) Solvent gradient operation of simulated moving beds. 2. Langmuir isotherms. *J. Chromatogr. A*, **1026** (1–2), 47–55.

29 Ziomek, G., Kaspereit, M., Jezowski, J.J., Seidel-Morgenstern, A., and Antos, D. (2005) Effect of mobile phase composition on the SMB processes efficiency stochastic optimization of isocratic and gradient operation. *J. Chromatogr. A*, **1070** (1–2), 111–124.

30 Pålsson, E., Gustavsson, P.-E., and Larsson, P.-E. (2000) Pellicular expanded bed matrix suitable for high flow rates. *J. Chromatogr. A*, **878**, 17–25.

31 Asghari, F., Jahanshahi, M., and Ghoreyshi, A.A. (2012) Preparation and characterization of agarose-nickel nanoporous composite particles customized for liquid expanded bed

adsorption. *J. Chromatogr. A*, **1242**, 35–42.

32 Asghari, F. and Jahanshahi, M. (2012) Fabrication and evaluation of low-cost agarose–zinc nanoporous composite matrix: influence of adsorbent density and size distribution on the performance of expanded beds. *J. Chromatogr. A*, **1257**, 89–97.

33 Hansson, M., Ståhl, S., Hjorth, R., Uhlén, M., and Moks, T. (1994) Single-step recovery of a secreted recombinant protein by expanded bed adsorption. *Biotechnology*, **12**, 285.

34 McCreath, G.E., Chase, H.A., and Lowe, C.R. (1994) Novel affinity separation based on perfluorocarbon emulsions: use of a perfluorocarbon affinity emulsion for the direct extraction of glucose-6-phosphate dehydrogenase from homogenized bakers' yeast. *J. Chromatogr. A*, **659**, 275–287.

35 Chang, Y.K., McCreath, G.E., and Chase, H.A. (1995) Development of an expanded bed technique for an affinity purification of G6PDH from unclarified yeast cell homogenates. *Biotechnol. Bioeng.*, **48** (4), 355–366.

36 McCreath, G.E., Chase, H.A., Owen, R.O., and Lowe, C.R. (1995) Expanded bed affinity chromatography of dehydrogenases from Bakers' yeast using dye-ligand perfluoropolymer supports. *Biotechnol. Bioeng.*, **48**, 341–354.

37 Garg, N., Galaev, I., and Mattiasson, B. (1996) Polymer-shielded dye-ligand chromatography of lactate dehydrogenase from porcine muscle in an expanded bed system. *Bioseparation*, **6**, 193–199.

38 Griffith, C.M., Morris, J., Robichaud, M., Annen, M.J., McCormick, A.V., and Flickinger, M.C. (1997) Fluidisation characteristics of and protein adsorption on fluoride-modified porous zirconium oxide particles. *J. Chromatogr. A*, **776**, 179–195.

39 Lewus, R.K. and Carta, G. (1999) Binary protein adsorption on gel-composite ion-exchange media. *AIChE J.*, **45** (3), 512–522.

40 Lihme, A., Zafirakos, E., Hansen, M., and Olander, M. (1999) Simplified and more robust EBA processes by elution in expanded bed mode. *Bioseparation*, **8**, 93–97.

41 Pai, A., Gondkar, S., and Lali, A. (2000) Enhance performance of expanded bed chromatography on rigid superporous adsorbent matrix. *J. Chromatogr. A*, **867**, 113–130.

42 Gondkar, S., Manudhane, K., Amritkar, N., Pai, A., and Lali, A. (2001) Effect of adsorbent porosity on performance of expanded bed chromatography of proteins. *Biotechnol. Prog.*, **17**, 522–529.

43 Tong, X.-D. and Sun, Y. (2001) Nd-Fe-B alloy-densified agarose gel for expanded bed adsorption of proteins. *J. Chromatogr. A*, **943**, 63–75.

44 Theodossiou, I., Elsner, H.D., Thomas, O.R.T., and Hobley, T.J. (2002) Fluidization and dispersion behavior of small high density pellicular expanded bed adsorbents. *J. Chromatogr. A*, **964**, 77–89.

45 Tong, X.-D. and Sun, Y. (2002) Particle size and density distributions of two dense matrices in an expanded bed system. *J. Chromatogr. A*, **977**, 173–183.

46 Dainiak, M.B., Galaev, I.Y., and Mattiasson, B. (2002) Polyelectrolyte-coated ion exchange for cell-resistant expanded bed adsorption. *Biotechnol. Prog.*, **18**, 815–820.

47 Tong, X.-D., Dong, X.-Y., and Sun, Y. (2002) Lysozyme adsorption and purification by expanded bed chromatography with a small-sized dense adsorbent. *Biochem. Eng. J.*, **12**, 117–124.

48 Jahanshahi, M., Pacek, A.W., Niewon, A.W., and Lyddiatt, A. (2003) Fabrication by three-phase emulsification of pellicular adsorbents customized for liquid fluidized bed adsorption of bioproducts. *J. Chem. Technol. Biotechnol.*, **78**, 1111–1120.

49 Li, P., Xiu, G., and Rodrigues, A.E. (2003) Modeling separation of proteins by inert core adsorbent in a batch adsorber. *Chem. Eng. Sci.*, **58**, 3361–3371.

50 Lei, Y.-L., Lin, D.-Q., Yao, S.-J., and Zhu, Z.-Q. (2003) Preparation and characterization of titanium oxide-densified cellulose beads for expanded bed adsorption. *J. Appl. Polym. Sci.*, **90**, 2848–2854.

51 Zhou, X., Shi, Q.-H., Bai, S., and Sun, Y. (2004) Dense pellicular agarose–glass beads for expanded bed application: fabrication and characterization for effective protein adsorption. *Biochem. Eng. J.*, **18**, 81–88.

52 Lei, Y.-L., Lin, D.-Q., Yao, S.-J., and Zhu, Z.-Q. (2005) Preparation of an anion exchanger based on TiO_2-densified cellulose beads for expanded bed adsorption. *React. Funct. Polym.*, **62**, 169–177.

53 Miao, Z.-J., Lin, D.-Q., and Yao, S.-J. (2005) Preparation and characterization of cellulose–stainless steel powder composite particles customized for expanded bed application. *Ind. Eng. Chem. Res.*, **44**, 8218–8224.

54 Lin, D.-Q., Miao, Z.-J., and Yao, S.-J. (2006) Expansion and hydrodynamic properties of cellulose–stainless steel powder composite matrix for expanded bed adsorption. *J. Chromatogr. A*, **1107**, 265–272.

55 Xia, H.-F., Lin, D.-Q., and Yao, S.-J. (2007) Spherical cellulose–nickel powder composite matrix customized for expanded bed application. *J. Appl. Polym. Sci.*, **104**, 740–747.

56 Xia, H.-F., Lin, D.-Q., and Yao, S.-J. (2007) Preparation and characterization of macroporous cellulose–tungsten carbide composite beads for expanded bed applications. *J. Chromatogr. A*, **1175**, 55–62.

57 Xia, H.-F., Lin, D.-Q., and Yao, S.-J. (2008) Chromatographic performance of macroporous cellulose–tungsten carbide composite beads as anion-exchanger for expanded bed adsorption at high fluid velocity. *J. Chromatogr. A*, **1195**, 60–66.

58 Gao, D., Yao, S.-J., and Lin, D.-Q. (2008) Preparation and adsorption behavior of a cellulose-based, mixed-mode adsorbent with a benzylamine ligand for expanded bed applications. *J. Appl. Polym. Sci.*, **107**, 674–682.

59 Jahanshahi, M., Partida-Martinez, L., and Hajizadeh, S. (2008) Preparation and evaluation of polymer-coated adsorbents for the expanded bed recovery of protein products from particulate feedstocks. *J. Chromatogr. A*, **1203**, 13–20.

60 Song, H.-B., Xiao, Z.-F., and Yuan, Q.-P. (2009) Preparation and characterization of poly glycidyl methacrylete-zirconium dioxide-β-cyclodextrin composite matrix for separation of isoflavones through expanded bed adsorption. *J. Chromatogr. A*, **1216**, 5001–5010.

61 Zhao, J., Lin, D.-Q., and Yao, S.-J. (2009) Expansion and hydrodynamic properties of β-cyclodextrin polymer/tungsten carbide composite matrix in an expanded bed. *J. Chromatogr. A*, **1216**, 7840–7845.

62 Zhao, J., Lin, D.-Q., Wang, Y.-C., and Yao, S.-J. (2010) A novel β-cyclodextrin polymer/tungsten carbide composite matrix for expanded bed adsorption: preparation and characterization of physical properties. *Carbohydr. Polym.*, **80**, 1085–1090.

63 Lihme, A., Hansen, M.B., Andersen, I.V., and Burnouf, T. (2010) A novel core fractionation process of human plasma by expanded bed adsorption chromatography. *Anal. Biochem.*, **399**, 102–109.

64 Shi, F., Lin, D.-Q., Phottraithip, W., and Yao, S.-J. (2011) Preparation of cellulose–tungsten carbide composite beads with ionic liquid for expanded bed application. *J. Appl. Polym. Sci.*, **119**, 3453–3461.

65 Lin, D.-Q., Tong, H.-F., van de Sandt, E.J. A.X., den Boer, P., Golubović, M., and Yao, S.-J. (2013) Evaluation and characterization of axial distribution in expanded bed. I. Bead size, bead density and local bed voidage. *J. Chromatogr. A*, **1304**, 78–84.

66 Zhan, X.-Y., Lu, D.-P., Lin, D.-Q., and Yao, S.-J. (2013) Preparation and characterization of supermacroporous polyacrylamide cryogel beads for biotechnological application. *J. Appl. Polym. Sci.*, **130** (5), 3082–3089.

67 Thömmes, J., Weiher, M., Karau, A., and Kula, M.-R. (1995) Hydrodynamics and performance in fluidized bed adsorption. *Biotechnol. Bioeng.*, **48**, 367–374.

68 Thömmes, J., Halfar, M., Lenz, S., and Kula, M.-R. (1995) Purification of monoclonal antibodies from whole hybridoma fermentation broth by fluidized bed adsorption. *Biotechnol. Bioeng.*, **45** (3), 205–211.

69 Chase, H.A. and Chang, Y.K. (1996) Ion exchange purification of G6PDH from unclarified yeast cell homogenates using expanded bed adsorption. *Biotechnol. Bioeng.*, **49**, 204–216.

70 Chase, H.A. and Chang, Y.K. (1996) Development of operating conditions for protein purification using expanded bed techniques: the effect of the degree of bed expansion on adsorption performance. *Biotechnol. Bioeng.*, **49**, 512–526.

71 Karau, A., Benken, C., Thommes, J., and Kula, M.-R. (1997) The influence of particle size distribution and operating conditions on the adsorption performance in fluidized beds. *Biotechnol. Bioeng.*, **55**, 54–64.

72 Smith, M.P. (1997) An evaluation of expanded bed adsorption for the recovery of protein from crude feedstock. PhD thesis. University College London, UK.

73 Finette, G.M.S., Baharin, B., Mao, Q.M., and Hearn, M.T.W. (1998) Optimization considerations for the purification of α1-antitrypsin using silica-based ion-exchange adsorbents in packed and expanded beds. *Biotechnol. Prog.*, **14**, 286–293.

74 Lan, J.C.-W., Hamilton, G.E., and Lyddiatt, A. (1999) Physical and biochemical characterization of a simple intermediate between fluidized and expanded bed contactors. *Bioseparation*, **8**, 43–51.

75 Pai, A., Gondkar, S., Sundaram, S., and Lali, A. (1999) Expanded bed adsorption on supermacroporous cross-linked celulose matrix. *Bioseparation*, **8**, 131–138.

76 Bruce, L.J., Clemmitt, R.H., Nash, D.C., and Chase, H.A. (1999) Monitoring of adsorbate breakthrough curves within an expanded bed adsorption column. *J. Chem. Technol. Biotechnol.*, **74**, 264–269.

77 Thömmes, J. (1999) Investigations on protein adsorption to agarose-dextran composite media. *Biotechnol. Bioeng.*, **62** (3), 358–362.

78 Willoughby, N.A., Hjorth, R., and Titchener-Hooker, N.J. (2000) Experimental measurement of particle size distribution and voidage in an expanded bed adsorption system. *Biotechnol. Bioeng.*, **69** (6), 648–653.

79 Clemmitt, R.H. and Chase, H.A. (2000) Facilitated downstream processing of a histidine-tagged protein from unclarified histidine-tagged protein from unclarified *E. coli* homogenates using immobilized metal expanded-bed adsorption. *Biotechnol. Bioeng.*, **67** (2), 206–216.

80 Wright, P.R. and Glasser, B.J. (2001) Modeling mass transfer and hydrodynamics in fluidized-bed adsorption of proteins. *AIChE J.*, **47** (2), 474–488.

81 Hu, H.-B., Yao, S.J., and Zhu, Z.-Q. (2001) Study on adsorption performance of BSA in Streamline DEAE and DEAE Sepharose FF adsorbents. *Chem. Eng. (China)*, **29**, 37–41.

82 Fernández-Lahore, H.M., Lin, D.-Q., Hubbuch, J.J., Kula, M.-R., and Thömmes, J. (2001) The use of ion-selective electrodes for evaluating residence time distributions in expanded bed adsorption systems. *Biotechnol. Prog.*, **17**, 1128–1136.

83 Bruce, L.J. and Chase, H.A. (2001) Hydrodynamics and adsorption behavior within an expanded bed adsorption column studied using expanded-bed sampling. *Chem. Eng. Sci.*, **56**, 3149–3162.

84 Bruce, L.J. and Chase, H.A. (2002) The combined use of in-bed monitoring and an adsorption model to anticipate breakthrough during expanded bed adsorption. *Chem. Eng. Sci.*, **57**, 3085–3093.

85 Chen, W.-D., Tong, X.-D., Dong, X.-Y., and Sun, Y. (2003) Expanded bed adsorption of protein with DEAE spherodex M. *Biotechnol. Prog.*, **19**, 880–886.

86 Tong, X.-D., Xue, B., and Sun, Y. (2003) Modeling of expanded-bed protein adsorption by taking into account the axial particle size distribution. *Biochem. Eng. J.*, **16**, 265–272.

87 Yun, J., Yao, S.-J., Lin, D.-Q., Lu, M.-H., and Zhao, W.-T. (2004) Modeling axial distributions of adsorbent particle size and local voidage in expanded bed. *Chem. Eng. Sci.*, **59**, 449–457.

88 Yun, J., Lin, D.-Q., and Yao, S.-J. (2004) Variation of the axial dispersion along the bed height for adsorbents with a density difference and a log-normal size distribution in an expanded bed. *Ind. Eng. Chem. Res.*, **43**, 8066–8073.

89 Yun, J., Lin, D.-Q., Lu, M.-H., Zhong, L.-N., and Yao, S.-J. (2004) Measurement and modeling of axial distribution of adsorbent particles in expanded bed: taking into account the particle density difference. *Chem. Eng. Sci.*, **59**, 5873–5881.

90 Li, P., Xiu, G., and Rodrigues, A.E. (2005) Experimental and modeling study of protein adsorption in expanded bed. *AIChE J.*, **51** (11), 2965–2977.

91 Yun, J., Lin, D.-Q., and Yao, S.-J. (2005) Predictive modeling of protein adsorption along the bed height by taking into account the axial nonuniform liquid dispersion and particle classification in expanded beds. *J. Chromatogr. A*, **1095**, 16–26.

92 Li, P., Xiu, G., Mata, V.G., Grande, C.A., and Rodrigues, A.E. (2006) Expanded bed adsorption/desorption of proteins with Streamline Direct CST I adsorbent. *Biotechnol. Bioeng.*, **94** (6), 1155–1163.

93 Chow, Y.M., Tey, B.T., Ibrahim, M.N., Ariff, A., and Ling, T.C. (2006) The performance of anion exchange expanded bed adsorption chromatography on the recovery of G6PDH from unclarified feedstock with high biomass concentration. *Biotechnol. Bioprocess Eng.*, **11**, 466–469.

94 Xia, H.-F., Lin, D.-Q., and Yao, S.-J. (2007) Evaluation of new high density ion exchange adsorbents for expanded bed adsorption chromatography. *J. Chromatogr. A*, **1145**, 58–66.

95 Chang, Y.-K., Chou, S.-Y., Liu, J.-L., and Tasi, J.-C. (2007) Characterization of BSA adsorption on mixed mode adsorbent. I. Equilibrium study in a well-agitated contactor. *Biochem. Eng. J.*, **35**, 56–65.

96 Poulin, F., Jacquemart, R., De Crescenzo, G., Jolicoeur, M., and Legros, R. (2008) A study of the interaction of HEK-293 cells with streamline chelating adsorbent in expanded bed operation. *Biotechnol. Prog.*, **24**, 279–282.

97 Lin, D.-Q., Chen, C.-Q., Wu, Y.-C., and Yao, S.-J. (2009) Separation of lactoferrin from whey by expanded bed adsorption with mixed-mode adsorbent. *J. Zhejiang Univ. (Eng. Sci.)*, **43** (3), 472–476.

98 Li, J. and Chase, H.A. (2009) Use of expanded bed adsorption to purify flavonoids from *Ginkgo biloba* L. *J. Chromatogr. A*, **1216**, 8759–8770.

99 Yap, W.B., Tey, B.T., Alitheen, N.B.M., and Tan, W.S. (2010) Purification of His-tagged hepatitis B core antigen from unclarified bacterial homogenates using immobilized metal affinity-expanded bed adsorption chromatography. *J. Chromatogr. A*, **1217**, 3473–3480.

100 Niu, J.F., Chen, Z.-F., and Wang, G.-C. (2010) Purification of phycoerythrin from *Porphyra yezoensis* Ueda (Bangiales, Rhodophyta) using expanded bed absorption. *J. Appl. Phycol.*, **22**, 25–31.

101 Shahavi, M.H., Jahanshahi, M., Najafpour, G.D., Ebrahimpour, M., and Hosenian, A.H. (2011) Expanded bed adsorption of biomolecules by NBG contactor: experimental and mathematical investigation. *World Appl. Sci. J.*, **13** (2), 181–187.

102 Alibolandi, M. and Mirzahoseini, H. (2011) Purification and refolding of overexpressed human basic fibroblast growth factor in *Escherichia coli*. *Biotechnol. Res. Int.* doi: 10.4061/2011/973741

103 Boeris, V., Balce, I., Vennapusa, R.R., Rodriguez, M.A., Picó, G., and Lahore, M.F. (2012) Production, recovery and purification of a recombinant β-galactosidase by expanded bed anion exchange adsorption. *J. Chromatogr. A*, **900**, 32–37.

104 Kelly, W., Garcia, P., McDemott, S., Mullen, P., Kamguia, G., Jones, G., Ubiera, A., and Göklen, K. (2013) Experimental characterization of next-generation expanded-bed adsorbents for capture of a recombinant protein expressed in high-cell-density yeast fermentation. *Biotechnol. Appl. Biochem.* doi: 10.0002/bab.1133

105 Moraes, C.C., Mazutti, M.A., Maugeri, F., and Kalil, S.J. (2013) Modeling of ion exchange expanded-bed chromatography for the purification of C-phycocyanin. *J. Chromatogr. A*, **1281**, 73–78.

106 Du, Q.-Y., Lin, D.-Q., Xiong, Z.-S., and Yao, S.-J. (2013) One-step purification of lactoferrin from crude sweet whey using cation-exchange expanded bed adsorption. *Ind. Eng. Chem. Res.*, **52**, 2693–2699.

107 den Boer, P., Doeven, M., van der Merwe, J., Lihme, A., Bendix-Hansen, M., Vaarst, I., Pontoppidan, M., and Linz, F. (2013) Rhobust EBA processing high-cell density mammalian cell cultures: process parameters and performance. DSM Biologics. Available at http://www.dsm.com/content/dam/dsm/pharmaceuticals/en_US/documents/ECCE%20Den%20Haag%20April%202013%20FINAL.pdf (last accessed October 16, 2013).

108 Kelly, W., Kamguia, G., Mullen, P., Ubiera, A., Göklen, K., Huang, Z., and Jones, G. (2013) Using two species competitive binding model to predict expanded bed breakthrough of a recombinant protein expressed in a high cell density fermentation. *Biotechnol. Bioprocess Eng.*, **18**, 546–559.

109 Johansson, B.L., Belew, M., Eriksson, S., Glad, G., Lind, O., Maloisel, L.J., and Norrman, N. (2003) Preparation and characterization of prototypes for multi-modal separation media aimed for capture of negatively charged bimolecular at high salt conditions. *J. Chromatogr. A*, **1016**, 21–33.

110 Johansson, B.L., Belew, M., Eriksson, S., Glad, G., Lind, O., Maloisel, L.J., and Norrman, N. (2003) Preparation and characterization of prototypes for multi-modal separation aimed for capture of positively charged biomolecules at high-salt conditions. *J. Chromatogr. A*, **1016**, 35–49.

111 Li, P., Xiu, G.H., and Rodrigues, A.E. (2003) Analytical breakthrough curves for inert core adsorbent with sorption kinetics. *AIChE J.*, **49** (11), 2974–2979.

112 Li, P., Yu, J.G., Xiu, G.H., and Rodrigues, A.E. (2010) A strategy for tailored design of efficient and low-pressure drop packed column chromatography. *AIChE J.*, **56** (12), 3091–3098.

113 Li, P., Yu, J.G., Xiu, G.H., and Rodrigues, A.E. (2011) Perturbation chromatography with inert core adsorbent: moment solution for two-component nonlinear isotherm adsorption. *Chem. Eng. Sci.*, **66** (20), 4555–4560.

114 Willoughby, N., Habib, G., Hoare, M., Hjorth, R., and Titchener-Hooker, N.J. (2000) The use of rapid on-line monitoring of products and contaminants from within an expanded bed to control separations exhibiting fast breakthrough characteristics and to maximize productivity. *Biotechnol. Bioeng.*, **70**, 254–261.

115 Chen, W.D., Dong, X.Y., and Sun, Y. (2003) Modeling of the whole expanded-bed protein adsorption process with yeast cell suspensions as feedstock. *J. Chromatogr. A*, **1012**, 1–10.

116 Kaczmarski, K. and Bellot, J.C. (2004) Theoretical investigation of axial and local particle size distribution on expanded bed adsorption process. *Biotechnol. Prog.*, **20**, 786–792.

117 Skidmore, G.L. and Chase, H.A. (1990) 2-Component protein adsorption to the cation exchanger S-Sepharose-FF. *J. Chromatogr. A*, **505**, 329–347.

118 Weinbrenner, W.F. and Etzel, M.R. (2004) Competitive adsorption of alpha-lactalbumin and bovine serum-albumin to a sulfopropyl ion-exchange membrane. *J. Chromatogr. A*, **662**, 414–419.

119 Martin, C., Iberer, G., Ubiera, A., and Carta, G. (2005) Two-component protein adsorption kinetics in porous ion exchange media. *J. Chromatogr. A*, **1079**, 105–115.

120 Hubbuch, R., Linden, T., Knieps, E., Thömmes, J., and Kula, M.R. (2003) Mechanism and kinetics of protein transport in chromatographic media studied by confocal laser scanning microscopy – Part II. Impact on chromatographic separations. *J. Chromatogr. A*, **1021**, 105–115.

121 Li, P., Xiu, G.H., and Rodrigues, A.E. (2007) Proteins separation and

purification by salt gradient ion-exchange SMB. *AIChE J.*, **53** (9), 2419–2431.

122 Jensen, T.B. (2003) Gradient SMB chromatography. PhD thesis. Kluyver Laboratory for Biotechnology, Delft University of Technology.

123 Mazzotti, M., Storti, G., and Morbidelli, M. (1997) Optimal operation of simulated moving bed units for nonlinear chromatographic separations. *J. Chromatogr. A*, **769** (1), 3–24.

124 Azevedo, D.C.S. and Rodrigues, A.E. (2001) Fructose–glucose separation in a SMB pilot unit: modeling, simulation, design and operation. *AIChE J.*, **47** (9), 2024–2051.

125 Minceva, M. and Rodrigues, A.E. (2005) Two-level optimization of an existing SMB for *p*-xylene separation. *Comput. Chem. Eng.*, **29** (10), 2215–2228.

126 Rodrigues, A.E. and Pais, L.S. (2004) Design of SMB chiral separations using the concept of separation volume. *Sep. Sci. Technol.*, **39** (2), 245–270.

127 Li, P., Yu, J.G., Xiu, G.H., and Rodrigues, A.E. (2008) Separation region and strategies for proteins separation by salt gradient ion-exchange SMB. *Sep. Sci. Technol.*, **43** (1), 11–28.